Phytoplankton Community Structure in Gulf Stream Mesoscale Eddies: A SWOT + PACE Satellite Data Fusion Approach

Jerry Chen, Lilian Dove
School of Earth & Atmospheric Sciences, Georgia Institute of Technology

Introduction

Phytoplankton are the foundation of marine food webs and contribute roughly 46% of global net primary production (Field et al., 1998). From past satellite altimetry studies, mesoscale eddies are known to shape phytoplankton biomass (Gaube et al., 2013; McGillicuddy, 2016), but bulk chlorophyll cannot distinguish which functional types are responding

Because different phytoplankton communities contribute differently to carbon export (Guidi et al., 2016), resolving community composition within eddies is important for connecting mesoscale dynamics to the biological carbon pump.

The overlapping SWOT and PACE satellite missions make it possible to move beyond bulk chlorophyll. SWOT's fine-scale altimetry enables improved eddy detection and tracking (Fu et al., 2024), while PACE's hyperspectral imaging supports pigment retrieval and phytoplankton functional type decomposition (Werdell et al., 2019). Together, these instruments shift eddy biogeochemistry from individual case studies to larger-scale analysis across the global oceans.

Study Region & Data

The study region spans the Gulf Stream in the Northwest Atlantic (29-44°N, 81-56°W), where coincident SWOT and PACE observations capture ocean topography and surface reflectance.

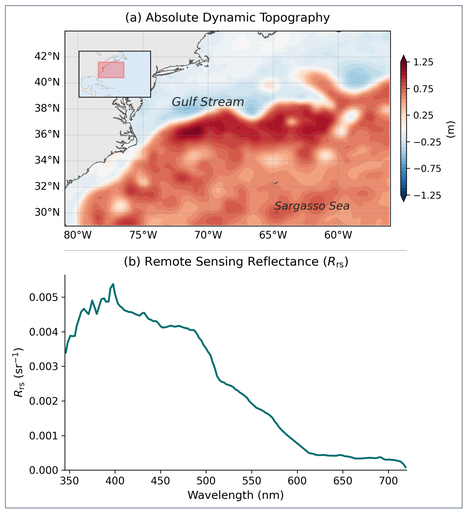

Figure 1. Snapshots of ADT and domain-averaged reflectance on March 12, 2025.

Methods Overview

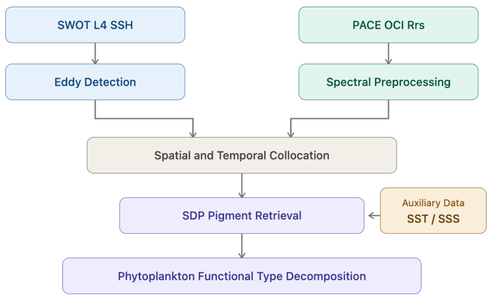

Figure 2. Data retrieval and fusion pipeline.

Methods: Eddy Detection & Tracking

We use py-eddy-tracker (PET) software to identify and track mesoscale eddies. Over the study period (Oct 2024 - Jul 2025), we identified 44 cyclonic and 35 anticyclonic long-lived eddy tracks (> 60 days).

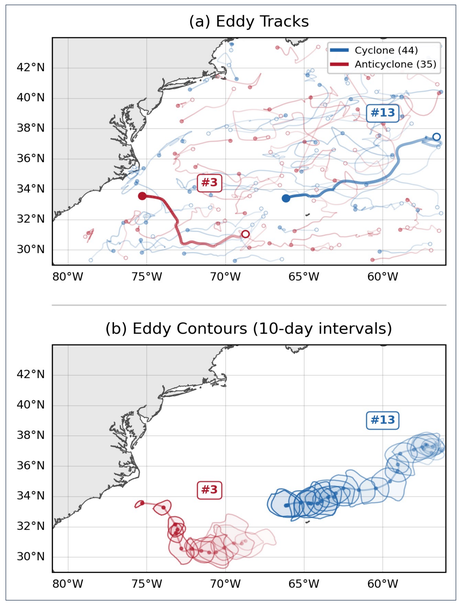

Figure 3. (a) Trajectories of all identified cyclonic (blue, n=44) and anticyclonic (red, n=35) eddies, with one representative eddy of each type highlighted. Hollow and filled circles mark the start and end positions, respectively. (b) Effective contours of the two highlighted eddies shown at 10-day intervals. Center positions at each interval are marked with dots.

Methods: PACE Collocation & Modeling

For each daily eddy snapshot, we extract PACE Rrs pixels within the eddy contour. Snapshots with a coverage score below 0.8 are discarded.

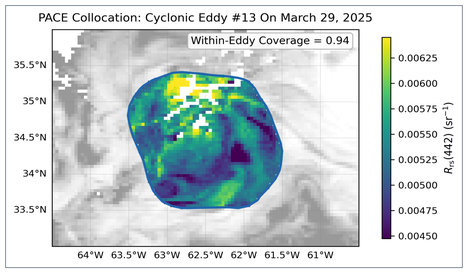

Figure 4. Pixels inside the eddy contour (blue) are retained for pigment analysis. Within-eddy coverage denotes the fraction of observations passing QA. White pixels indicate missing pixel values that did not pass QA.

At each pixel, diagnostic pigment concentrations were modeled using the spectral decomposition approach (Kramer et al., 2022). PFTs were quantified using the phytoclass algorithm (Hayward et al., 2023).

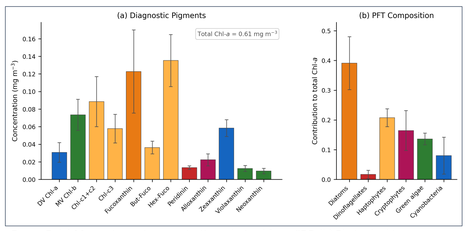

Figure 5. (a) Mean pigment concentrations derived from SDP. (b) Phytoplankton functional type contributions to total Chl-a derived from phytoclass.

Results: PFT By Eddy Polarity

Cyclonic eddies show pronounced right tails for most phytoplankton functional types except cyanobacteria. Anticyclonic eddies show low productivity except for cyanobacteria, where concentrations are roughly normally distributed in both polarities.

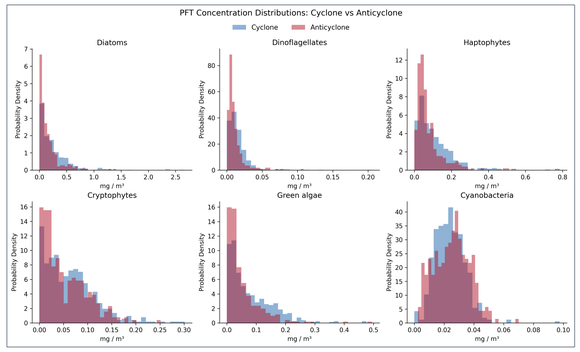

Figure 6. Density-normalized distributions of PFT concentrations in cyclonic and anticyclonic eddies. Each observation is the spatial mean within one eddy on one PACE observation date.

Results: Radial PFT Structure

Three PFTs show polarity-dependent differences that persist from the eddy core throughout the effective eddy radius. Diatoms and green algae are enriched in cyclones by 10-15% of the pairwise mean, while cyanobacteria are depleted in cyclones by roughly 30%.

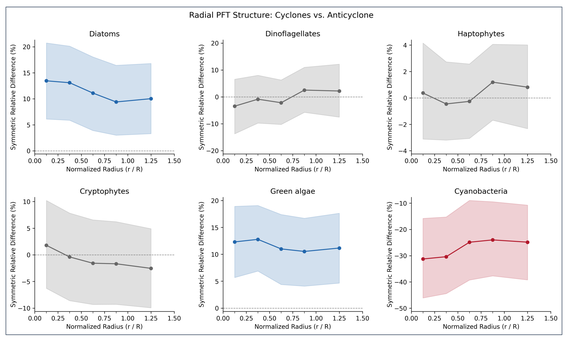

Figure 7. Symmetric relative percent difference ($\frac{2(cyc-anti)}{cyc+anti} \times 100\%$) in PFT contribution to total Chl-a across 5 normalized radial bins (r/R, where R is effective eddy radius). Shaded intervals are 95% bootstrap confidence intervals from 1000 resamples. Color indicates whether Cis exclude 0 at each bin (blue: cyclone-enriched, red: cyclone-depleted, gray: inconclusive).

Results: Seasonal Trends Across Eddies

Both eddy polarities show seasonal increases in total chlorophyll a from fall to spring, with cyclones maintaining higher mean values than anticyclones across most months with larger variability.

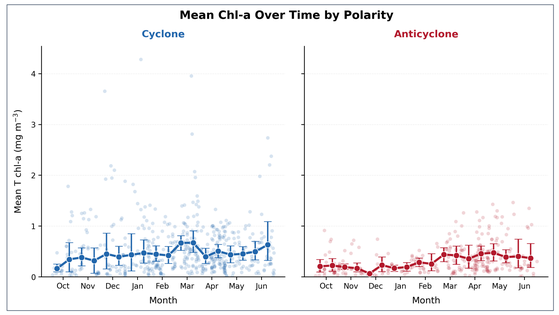

Figure 8. Total chlorophyll a is aggregated across eddies, first spatially for each daily snapshot and then temporally across a half-month bin. Mean values are plotted with 95% confidence intervals. Individual eddy-date means are plotted with positions relative to observation date within each bin.

Discussion of Results

Eddy pumping drives community shifts

- In the Northern Hemisphere, cyclonic eddies generate upwelling of nutrient-rich water into the euphotic zone, favoring fast-growing diatoms and green algae.
- Anticyclonic eddies produce downwelling, which suppresses new production, selecting for cyanobacteria which are well-adapted for oligotrophic waters.

Productivity shifts due to polarity are eddy-wide, not just at the core

- Since cyclonic upwelling/downwelling occurs near the core, we expect the contrast between cyclonic and anticyclonic eddies to peak near the center of the eddy. However, there is no significant difference in PFT quantities between cyclonic/anticyclonic eddies at the center vs. edges.

Eddy PFTs vary seasonally

- Cyclonic and anticyclonic eddies did not significantly differ in seasonal trends for total chlorophyll.
- Cyclonic eddies consistently show not only higher total chlorophyll, but also greater variability, particularly during the spring bloom period.

Conclusions

1. Eddy polarity is a strong influencer of phytoplankton composition and biomass.
Cyclonic eddies are more biologically productive than anticyclonic eddies, with higher chlorophyll and increased amounts of diatoms and green algae. Cyanobacteria thrive in anticyclones under oligotrophic conditions.

2. Satellite synergy unlocks population-scale BGC analysis of eddies.
Pairing SWOT altimetry with PACE hyperspectral Rrs makes it possible to move beyond individual case studies and quantify phytoplankton patterns across many eddies over broader spatial and temporal scales. The new datasets allow for capturing both physical structure and biological variability, enabling more detailed regional analysis of eddy-driven ecosystem change.

Next Steps

Even as improved satellite datasets increase our ability to identify, track, and quantify changes in eddies on a larger scale, the high percentage of cloud cover makes it difficult to track changes in the same eddy on a daily timescale.

Future work involves developing an algorithm to pool data across eddies in the same region by polarity, season, and location of origin to better understand the temporal evolution of phytoplankton within eddies throughout their lifetime.

References

- Field, C. B., Behrenfeld, M. J., Randerson, J. T., & Falkowski, P. (1998). Primary production of the biosphere: Integrating terrestrial and oceanic components. Science, 281(5374), 237–240. https://doi.org/10.1126/science.281.5374.237
- Fu, L.-L., Pavelsky, T., Crétaux, J.-F., Morrow, R., Farrar, J. T., Vaze, P., Sengenes, P., Vinogradova-Shiffer, N., Sylvestre-Baron, A., Picot, N., & Dibarboure, G. (2024). The Surface Water and Ocean Topography Mission: A breakthrough in radar remote sensing of the ocean and land surface water. Geophysical Research Letters, 51(4), e2023GL107652. https://doi.org/10.1029/2023GL107652
- Gaube, P., Chelton, D. B., Strutton, P. G., & Behrenfeld, M. J. (2013). Satellite observations of chlorophyll, phytoplankton biomass, and Ekman pumping in nonlinear mesoscale eddies. Journal of Geophysical Research: Oceans, 118, 6349–6370. https://doi.org/10.1002/2013JC009027
- Guidi, L., Chaffron, S., Bittner, L., Eveillard, D., Larhlimi, A., Roux, S., Darzi, Y., Audic, S., Berline, L., Brum, J. R., Coelho, L. P., Espinoza, J. C. I., Malviya, S., Sunagawa, S., Dimier, C., Kandels-Lewis, S., Picheral, M., Poulain, J., Searson, S., . . . Gorsky, G. (2016). Plankton networks driving carbon export in the oligotrophic ocean. Nature, 532(7600), 465–470. https://doi.org/10.1038/nature16942
- Hayward, A., Pinkerton, M. H., & Gutierrez-Rodriguez, A. (2023). phytoclass: A pigment-based chemotaxonomic method to determine the biomass of phytoplankton classes. Limnology and Oceanography: Methods, 21(4), 220–241. https://doi.org/10.1002/lom3.10541
- Kramer, S. J., Siegel, D. A., Maritorena, S., & Catlett, D. (2022). Modeling surface ocean phytoplankton pigments from hyperspectral remote sensing reflectance on global scales. Remote Sensing of Environment, 270, 112879. https://doi.org/10.1016/j.rse.2021.112879
- McGillicuddy, D. J., Jr. (2016). Mechanisms of physical-biological-biogeochemical interaction at the oceanic mesoscale. Annual Review of Marine Science, 8, 125–159. https://doi.org/10.1146/annurev-marine-010814-015606
- Werdell, P. J., Behrenfeld, M. J., Bontempi, P. S., Boss, E., Cairns, B., Davis, G. T., Franz, B. A., Gliese, U. B., Gorman, E. T., Hasekamp, O. P., Knobelspiesse, K. D., Mannino, A., Martins, J. V., McClain, C. R., Meister, G., & Remer, L. A. (2019). The Plankton, Aerosol, Cloud, ocean Ecosystem (PACE) mission: Status, science, advances. Bulletin of the American Meteorological Society, 100(9), 1775–1794. https://doi.org/10.1175/BAMS-D-18-0056.1